NRC Research Press

NOTE

Soil consistency and interparticle characteristics of xanthan gum biopolymer–containing soils with pore-fluid variation

Ilhan Chang, Yeong-Man Kwon, Jooyoung Im, and Gye-Chun Cho

Abstract: Biopolymer–soil technology is currently recognized as an environmentally friendly soil improvement method for geotechnical engineering practices. However, concerns exist regarding biopolymer fine-soil applications because the performance of biopolymers is based on an electrical interaction with clay or a pore fluid. Thus, the effect of water content and pore-fluid chemistry on biopolymer behavior in soil must first be clarified in terms of biopolymer applications. In this study, the liquid limits of xanthan gum biopolymer–treated clay–sand mixtures (clayey silt, kaolinite, montmorillonite, and sand) were obtained using three chemically distinct pore fluids (deionized water, 2 mol/L NaCl brine, and kerosene). Xanthan gum has contrary effects to the soil consistency, where the liquid limit can decrease via xanthan gum–induced particle aggregation or increase due to xanthan gum hydrogel formation. The clay-mineral type governed the xanthan gum behavior in the deionized water, while the pore-fluid chemistry governed the xanthan gum behavior in the brine and the kerosene.

Key words: xanthan gum biopolymer, pore-fluid chemistry, electrical sensitivity, soil classification, liquid limit.

Résumé : La technologie des biopolymères des sols est reconnue de nos jours comme une méthode d'amélioration des sols respectueuse de l'environnement pour les pratiques d'ingénierie géotechnique. Toutefois, les applications de biopolymères dans les sols fins suscitent des préoccupations, car les performances des biopolymères reposent sur une interaction électrique avec de l'argile ou un fluide interstitiel. Ainsi, l'effet de la teneur en eau et de la chimie des liquides interstitiels sur le comportement des biopolymères dans le sol doit d'abord être clarifié en termes d'application de biopolymères. Dans cette étude, les limites liquides des mélanges argile-sable traités au biopolymère de gomme xanthane (limon argileux, kaolinite, montmorillonite et sable) ont été obtenues à l'aide de trois fluides interstitiels chimiquement distinctifs (eau désionisée, saumure 2 mol/L NaCl et kérosène). La gomme de xanthane a des effets contraires à la consistance du sol, la limite de liquidité pouvant diminuer en raison de l'agrégation de particules induite par la gomme de xanthane ou à son augmentation en raison de la formation d'hydrogel de gomme de xanthane. Le type argilo-minéral régit le comportement de la gomme de xanthane dans l'eau désionisée, tandis que la chimie des liquides interstitiels régit le comportement de la gomme de xanthane dans la saumure et le kérosène. [Traduit par la Rédaction]

Mots-clés : biopolymère de gomme de xanthane, chimie de fluide interstitiel, sensibilité électrique, classification des sols, limite de liquidité.

Introduction

The use of exocultured biological materials, known as "biopolymers", has been introduced to overcome the limitations of microbe endocultivation in soil in the form of a newly utilized environmentally friendly construction material for geotechnical engineering applications (Chang et al. 2016a; Latifi et al. 2017).

Recent studies have reported a promising biopolymer effect that improves the strength and stability of soils (Chang et al. 2016b; Ferruzzi et al. 2000; Orts et al. 2007). Microbial biopolymers show erosion reduction against surface water runoff in waterfronts (Ham et al. 2016, 2018) and agricultural farm lands (Orts et al. 2000), while strengthening and interparticle interaction behaviors of the polysaccharide-type biopolymers, such as dextran, beta-glucan, xanthan gum, and gellan gum, with different soil types have been investigated by many researchers (Chang and Cho 2012, 2014; Chang et al. 2015a, 2015c, 2016b, 2017; Kwon and Ajo-Franklin 2013). Biopolymers synthesized from lignin, starch, and acrylamide can decrease the decomposition of plant residues

(Awad et al. 2012) or even promote vegetation growth in soils (Chang et al. 2015d). Moreover, biopolymers produced from food waste (e.g., bovine milk) can contribute to the reduction of dairy and relevant food waste (Chang et al. 2018). Furthermore, biopolymers can become an alternative earth construction binder in regions where ordinary cement is scarce and expensive, such as Africa (Chang et al. 2015b).

However, application of biopolymers to soil treatment requires considerations of the biopolymer rheology, phase transfer with water content variation, biopolymer to soil ratio, soil type, and pore-fluid condition, which affects the biopolymer–soil matrix formation (Chang and Cho 2019; Chang et al. 2015c, 2017). Biopolymer-treated soils with a high water content show low strength due to the low viscous biopolymer hydrocolloids surrounding soil particles (Chang et al. 2017), while dehydration increases the soil strength due to the condensation of the biopolymer hydrogels forming high-tensile-strength biofilms through the soil particulate network (Chang et al. 2016a). For biopolymer-treated sands, the concentration of biopolymer hydrogels be-

I. Chang. School of Engineering and Information Technology, University of New South Wales (UNSW), Canberra, ACT 2600, Australia.
Y.-M. Kwon, J. Im, and G.-C. Cho. Department of Civil and Environmental Engineering, Korea Advanced Institute of Science and Technology (KAIST), Daejeon 34141, Republic of Korea.
Corresponding author: Gye-Chun Cho (email: gyechun@kaist.edu).

Table 1. Basic properties of soils.

| Soil | D_{50} (μm) | SSA (m²/g)[a] | CEC (meq/100 g)[b] | PL (%) | LL_{DI} | LL_B | LL_K | USCS[c] | Clay-to-sand ratio | | |
									100:0	50:50	20:80
Jumunjin sand	421	—	—	—	—	—	—	SP	—	—	—
Clayey silt	12.5	2.2	—	23.8	30.5	28.8	32.1	ML	L10	L5S5	L2S8
Kaolinite	3	22.1	6.1	31	69.8	50.9	93.2	CH	K10	K5S5	K2S8
Montmorillonite	0.07[d]	220.6	64.1	61.6	398.5	94.2	60.5	CH	M10	M5S5	M2S8

[a]Specific surface area (SSA) obtained by the methylene blue adsorption method (Santamarina et al. 2001).
[b]Cation-exchange capacity (CEC) obtained by the methylene blue cation–exchange capacity method (Inglethorpe et al. 1993).
[c]Unified Soil Classification System (ASTM 2017b).
[d]Data obtained from Plaschke et al. (2001).

comes the dominant factor controlling the strength behavior of sands (Chang et al. 2016a; Lee et al. 2017). Meanwhile, electrostatic and chemical bonding characteristics between biopolymers and clayey particles become important for fine soils, where the "biopolymer-to-clay content" (in mass) becomes more critical than the "biopolymer-to-total soil content" (in mass) in terms of the strengthening purpose for biopolymer-treated soils (Chang and Cho 2019; Chang et al. 2015a).

Soil consistency (plastic limit; PL; liquid limit, LL; and plasticity index, PI) not only indicates the soil–water interaction on the particle surfaces, but also represents the pore-fluid chemical environment in pore spaces (Jang and Santamarina 2016). Biopolymer-treated soils show different LL behaviors, where the presence of biopolymer can increase (hydrogel swelling) or decrease (via particle aggregation) the LL of soils (Chang and Cho 2014; Nugent et al. 2009).

Xanthan gum is one of the most common biopolymers used in geotechnical engineering applications, such as soil stabilization (Chang et al. 2015a; Im et al. 2017; Latifi et al. 2017; Lee et al. 2017), mine tailings treatment (Chen et al. 2015), erosion control (Qureshi et al. 2017), adobe buildings (Chang et al. 2015b; Dove et al. 2016), and permeability control (Cabalar et al. 2017; Martin et al. 1996). However, most studies have focused on the macrobehavior of xanthan gum–treated soils without detailed consideration of the microscale soil–fluid interaction. The particle aggregation and water absorption characteristics of xanthan gum hydrogels seem to mainly affect the geotechnical behavior of fine soils. Thus, this study aims to investigate soil behaviors when xanthan gum hydrogels become the main pore-filling medium. Specifically, the effect of xanthan gum on soil consistency are evaluated through laboratory tests under different pore-fluid conditions.

Materials and methods

Materials

Sand: jumunjin sand

"Jumunjin" sand (standard sand material of Korea), which is a type of quartz-based (SiO₂) poorly graded sand (SP, classified in accordance with ASTM 2017b) (Kim et al. 2013), is used in this study. The surface of jumunjin sand is regarded to be electrically neutral; therefore, the interaction between jumunjin sand and biopolymer is not regarded to be influenced by the pore-fluid chemistry, while soil consistency is mainly governed by the clay fraction (Jang and Santamarina 2016).

Fine soils: clayey silt, kaolinite, and montmorillonite

Silt is known to have low plasticity development when mixed with water, where its LL and PL are mostly lower than those of clay (Mitchell and Soga 2005). The clayey silt used in this study is sampled from Danyang, Korea, and its basic properties are listed in Table 1.

Kaolinite clay is more hydrophilic than sand and silt, which forms strong hydrogen bonds with water molecules. However, as kaolinite has a stable 1:1 layer structure of gibbsite and silica

sheets, kaolinite becomes less sensitive to fluid chemistry than montmorillonite (Santamarina et al. 2001). Bintang kaolinite (CEC = 6.1 meq/100 g; Belitung Island, Indonesia) is used in this study (Table 1).

Montmorillonite is a smectite clay consisting of two layers of silica sheets and one layer of gibbsite with exchangeable cations (e.g., sodium or calcium) at interlayers, where a large amount of water can occupy the interlayer spaces and swell (Das 2013; Hensen and Smit 2002). The surface of montmorillonite is negatively charged by isomorphic substitutions, resulting in a high cation-exchange capacity (CEC) (Sondi et al. 1996) and an accompanying thick double layer (Taylor 1985), which renders the consistency of montmorillonite to be higher than kaolinite. A research grade montmorillonite material (CAS:1302-78-9, CEC = 64.1 meq/100 g; Sigma Aldrich) is used for this study (Table 1).

Fine soil–sand mixtures

The particle-size distribution (PSD) curves of soils used in this study are plotted in Fig. 1. To represent various sand–clay mixtures, jumunjin sand and fine soils (clayey silt, kaolinite, and montmorillonite) were mixed with 100% (pure fine soil), 50% (fine-based soil), and 20% (sand-based soil) clay contents, as summarized in Table 1.

Xanthan gum biopolymer

Xanthan gum is an anionic polysaccharide biopolymer produced by the *Xanthomonas campestris* bacterium. It is widely used as a thickener due to its viscous hydrogel formation with the presence of water (García-Ochoa et al. 2000). Research-grade xanthan gum from *Xanthomonas campestris* (CAS: 11138-66-2; Sigma Aldrich) is used in this study. The viscosity of 0.5% xanthan gum solution varies from 10 020 to 11 700 cps (1 cps = 1 mPa·s), depending on the shear rate (0.022~0.11 s⁻¹), as measured by a laboratory viscometer (Brookfield DV2TLV).

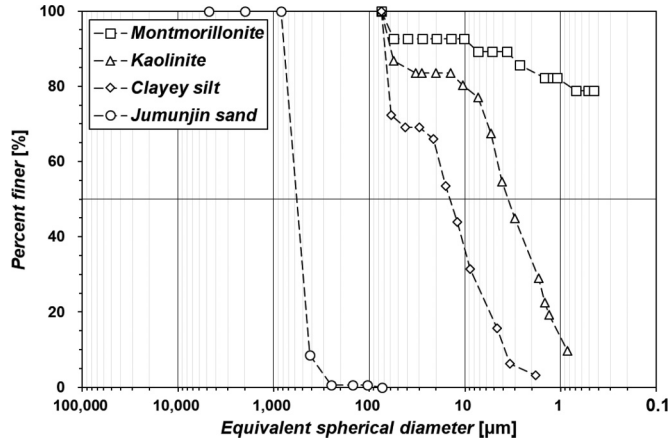#### Pore-fluids: deionized water, brine, and kerosene

Three distinct fluids —deionized water, brine, and kerosene — are used to investigate the effects on the variations in xanthan gum–soil interaction. The electric conductivity (σ_{el}) and relative permittivity (κ') distinguish pore-fluid chemistry. Deionized water ($\kappa' = 80$, $\sigma_{el} < 5$ μS/m, pH = 6.5) was obtained using the reverse-osmosis process. The brine solution ($\kappa' = 55$, $\sigma_{el} = 12$ S/m, pH = 6.5) was prepared by dissolving sodium chloride (CAS No. 1310-58-3; Junsei Chemical) into deionized water by using a magnetic stirrer to obtain a 2 mol/L NaCl solution. Common kerosene ($\kappa' = 2$, $\sigma_{el} = 10^{-11}$ S/m; GS Caltex) was used. The pH and σ_{el} of deionized water and 2 mol/L NaCl brine were measured with a pH/conductivity meter (S470-USP-K; Mettler Toledo), while the values of σ_{el} of kerosene and κ' of all fluids were obtained from Jang and Santamarina (2016).

Experimental program

Soil – xanthan gum mixture preparation

All soil materials (clayey silt, kaolinite, montmorillonite, and jumunjin sand) were dried in an oven at 105 °C for at least 24 h

Fig. 1. Particle-size distribution of soils used in this study.

Fig. 2. Liquid limit of xanthan gum–treated clayey silt – sand soils with variation in m_b/m_s (xanthan gum–to-soil content in mass): (*a*) deionized water pore fluid; (*b*) 2 mol/L NaCl brine pore fluid; (*c*) kerosene pore fluid.

before experimental procedures, according to ASTM D2216 (ASTM 2007). Then, each type of soil was thoroughly mixed with dry xanthan gum to obtain xanthan gum–soil mixtures with 0.1%, 0.5%, 1.0%, and 2.0% xanthan gum–to-soil mass content (m_b/m_s), while untreated soils (m_b/m_s = 0%) were prepared simultaneously.

Atterberg limit (PL and LL) measurements

The PL values of the soils were determined using a thread-rolling device (unglazed paper attached to the top and bottom plates with a controlled minimum spacing of 3.2 mm) to ensure consistent repeatability and reliability according to ASTM D4318 (ASTM 2017a). Five measurements were conducted for each soil condition to minimize measurement errors.

The LL values of soils were determined through a fall cone test (British Standards Institution 2017; Hansbo 1957; Koumoto and Houlsby 2001) by using a cone with a mass of 80 g and a tip angle of 30°, where the penetration depth was measured for 5 s by using a dial gauge with a precision of 0.01 mm. The LL values were determined according to the water content when the cone penetration was 20 mm into the soil sample. Other testing procedure details were followed by referring to BS EN ISO 17892-6:2017 (British Standards Institution 2017). Fall cone tests were repeated at least three times for a single soil condition to obtain reliable averages.
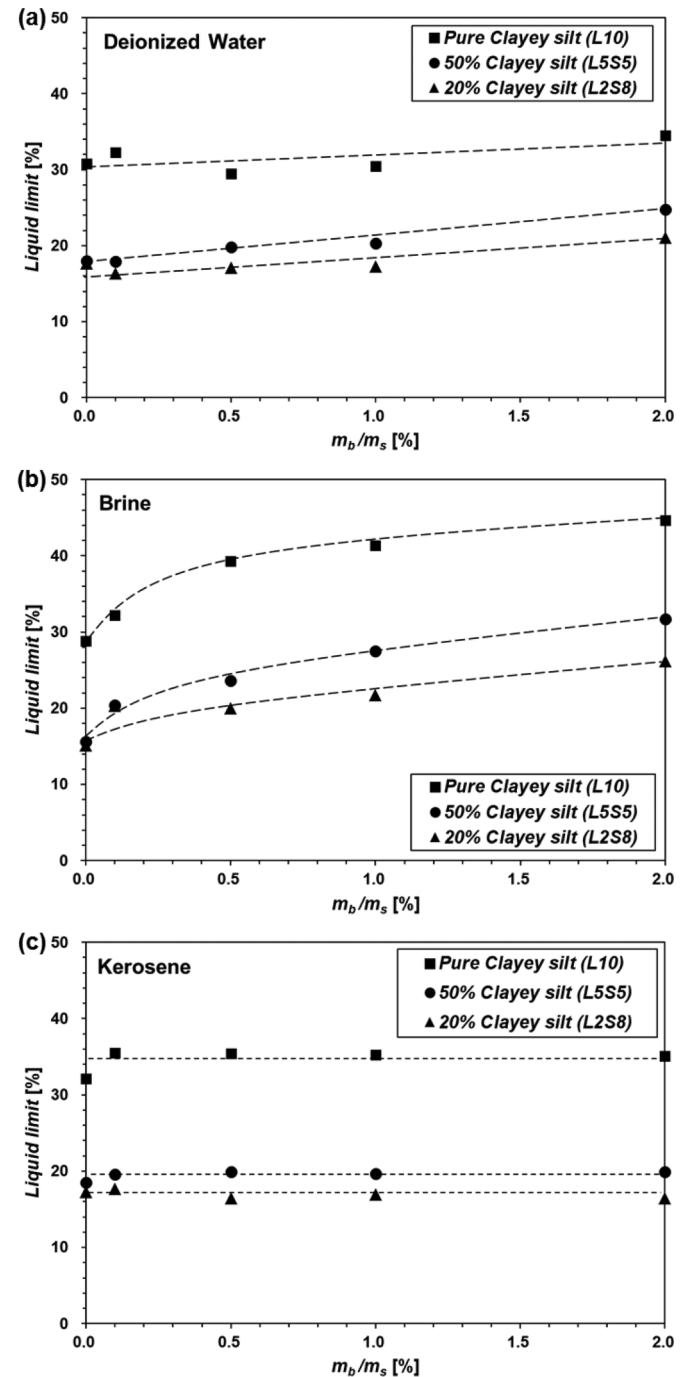
Results and analyses

The values of LL with deionized water (LL_{DI}), 2 mol/L NaCl brine (LL_B), and kerosene (LL_K) of xanthan gum–treated soils with variations in xanthan gum content are summarized in Figs. 2, 3, and 4 for clayey silt–sand, kaolinite–sand, and montmorillonite–sand soils, respectively. For all soil conditions, higher fine contents show higher LL values regardless of the pore-fluid condition.

LL behavior of untreated fine soils with pore-fluid variation

Particle–pore-fluid interactions of untreated fine-grained soils depend on particle mineralogy and pore-fluid chemistry (Jang and Santamarina 2016). The amount of water absorbed on the clay surface is affected by the amount of surface charge and particle size of clay minerals (Sridharan et al. 1986, 1988; White 1949), which alters the particle packing of clays (Chang and Cho 2010). Untreated clayey silt with low surface charges shows no significant change in LL values (i.e., LL_{DI}, LL_B, LL_K differences less than 3.5% for untreated clayey silt–sand soils) (Fig. 2). In contrast, clays are affected by the electrochemical property of pore fluids owing to active interaction of the surface charge with pore fluids.

Counter-ions in pore fluid decrease water adsorption of clay surfaces accompanying a decrease in double-layer thickness; thus, most clays exhibit the following relationship: $LL_{DI} > LL_B$ (Jang and Santamarina 2016; Mitchell and Soga 2005). As montmorillonite has a higher CEC than kaolinite, the $LL_{DI} \rightarrow LL_B$ reduction of
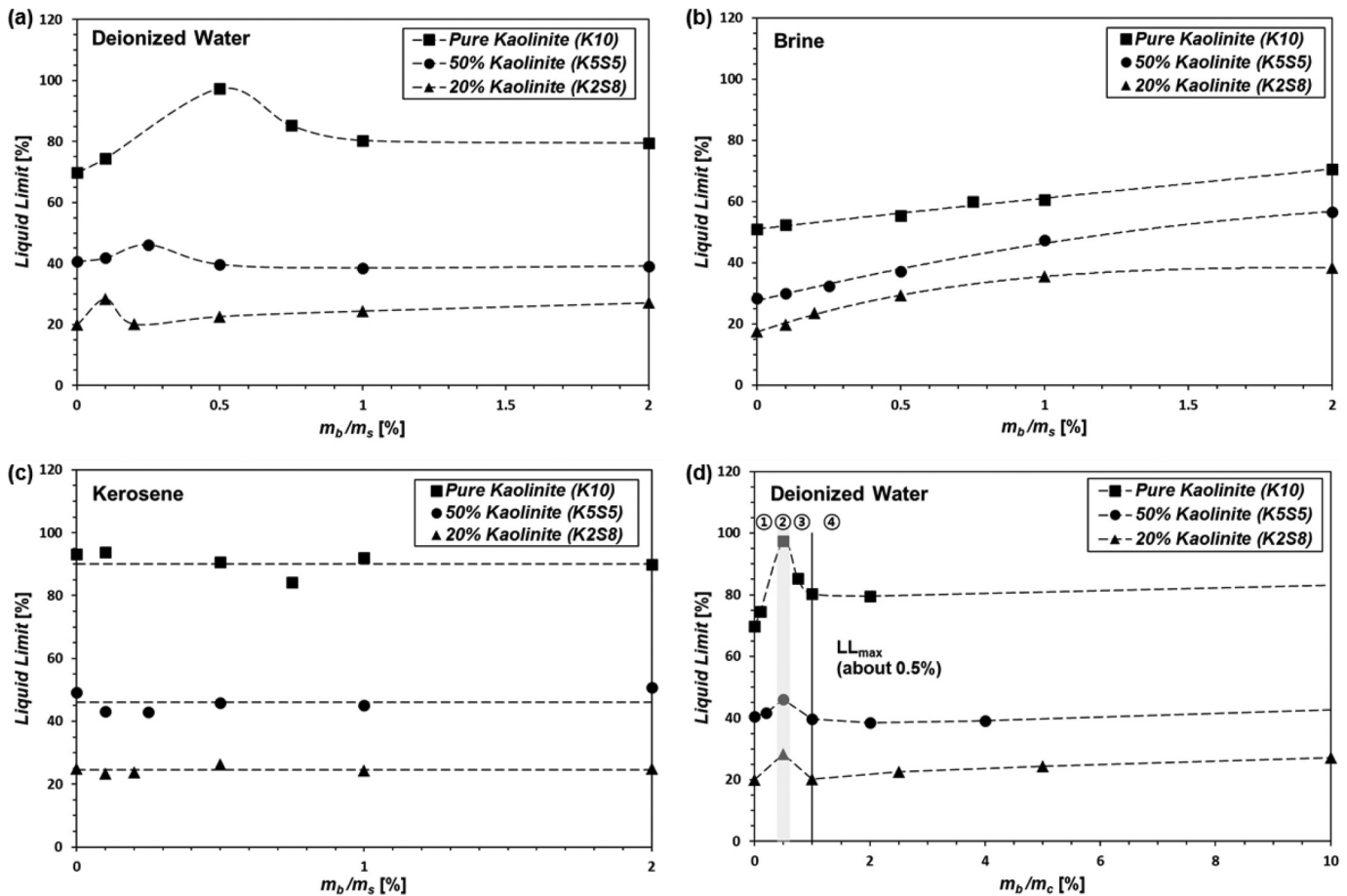
montmorillonite (Figs. 4a and 4b) is also larger than that of kaolinite (Figs. 3a and 3b).

Under a nonwetting pore-fluid condition (kerosene), edge charge and van der Waals forces dominantly affect particle–pore-fluid interactions (Jang and Santamarina 2016; Sridharan and Prakash 1999). Kaolinite has a higher proportion of edge charges (12%–36% of total area) than montmorillonite (<5% of total area), which results in $LL_{DI} < LL_K$ for kaolinite (Fig. 3), while montmorillonite shows $LL_{DI} \gg LL_K$ (Fig. 4) owing to the higher edge charge and van der Waals force interaction for kaolinite (Brady et al.

Fig. 3. Liquid limit of xanthan gum–treated kaolinite–sand mixtures with variations in m_b/m_s: (*a*) deionized water pore fluid; (*b*) 2 mol/L NaCl brine pore fluid; (*c*) kerosene pore fluid; (*d*) LL_{DI} with m_b/m_c (xanthan gum–to-clay content in mass) variation.

1996; Theng 2012; Tombácz and Szekeres 2006). The LL behaviors of untreated fine soils obtained from this study are in accordance with the findings of Jang and Santamarina (2016).

LL_{DI}, LL_B, and LL_K of xanthan gum–treated clayey silt–sand soils

For clayey silt–sand soils, xanthan gum mainly interacts with pore fluids in the form of hydrophilic hydrogel owing to negligible surface charges of silt and sand (Mitchell and Soga 2005), where xanthan gum hydrogel gradually increases both LL_{DI} (Fig. 2*a*) and LL_B (Fig. 2*b*) of clayey silt–sand soils with xanthan gum contents. The LL_K values remain constant, regardless of the content of xanthan gum (Fig. 2*c*).

LL_{DI}, LL_B, and LL_K of xanthan gum–treated kaolinite–sand soils

Kaolinite–sand soils show distinctive LL_{DI} behaviors where LL_{DI} varies with xanthan gum content increase, as shown in Figs. 3*a* and 3*d*. In particular, LL_{DI} initially increases (①) to a peak point (②; m_b/m_s = 0.5% for K10), decreases to an inflection point (③; m_b/m_s = 1.0% for K10), and then seems to remain constant up to m_b/m_s = 2% (④).
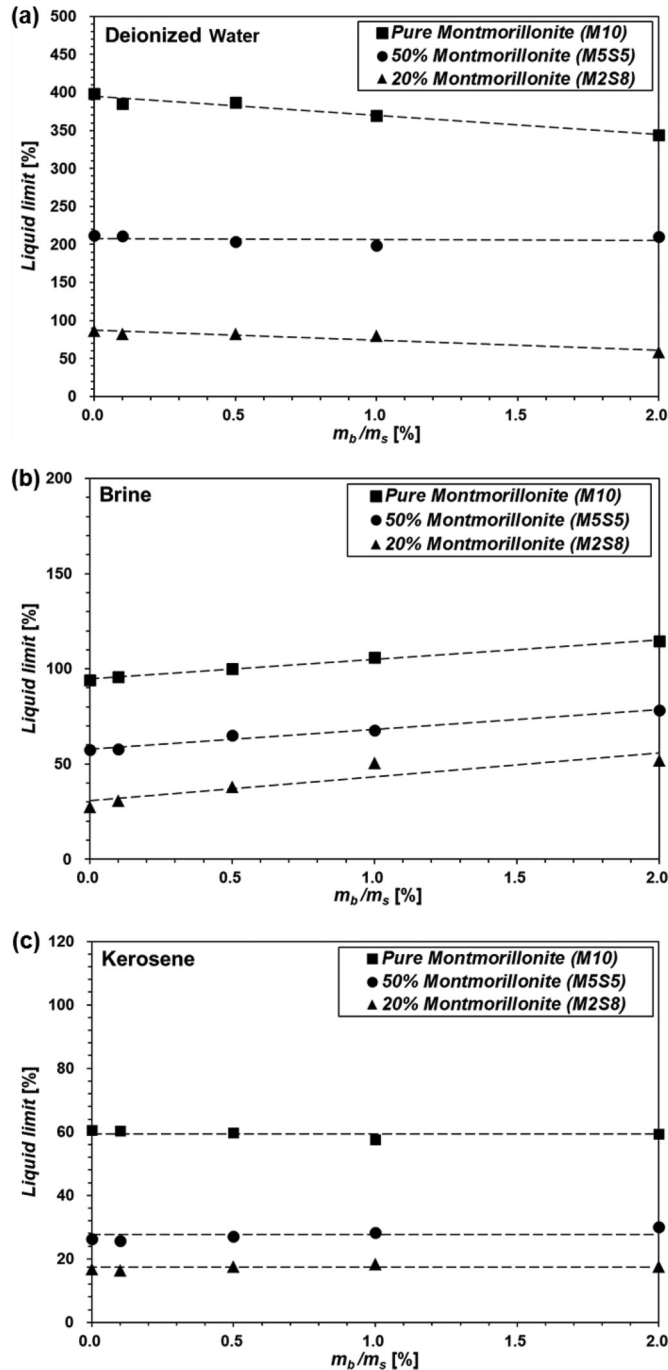
Figure 3*d* represents the variation in LL_{DI} in terms of xanthan gum–to-clay (kaolinite) mass content (m_b/m_c). Variation of LL_{DI} with m_b/m_c implies the hydrogel viscosity increase and particle aggregation effects induced by xanthan gum (Nugent et al. 2009). At low xanthan gum contents, xanthan gum instantly forms hydrogels, which results in the increase in LL_{DI}, as shown in ①; Fig. 3*d*. All kaolinite–sand soils show a peak LL_{DI} at m_b/m_c = 0.5%, which is in accordance with the previous finding from Chang and

Cho (2019) addressing m_b/m_c to mainly govern biopolymer–clay matrix formation and relevant shear strength properties (i.e., cohesion and friction angle) (Chang and Cho 2019). As the content of xanthan gum increases, xanthan gum initiates kaolinite aggregation via ionic or hydrogen bonding (Laird 1997; Sastry et al. 1995; Theng 2012), which accompanies a decrease in LL_{DI} (③ in Fig. 3*d*). The behavior of LL_{DI} for $m_b/m_c > 1\%$ (④; Fig. 3*d*) seems to be attributed to the equilibrium between xanthan gum hydrogel formation and the simultaneous kaolinite aggregation induced by xanthan gum (Nugent et al. 2009). Meanwhile, LL_B increases gradually with the content of xanthan gum (Fig. 3*b*). Xanthan gum shows no effect on the variation in LL_K (Fig. 3*c*), mainly due to the absence of xanthan gum hydrogel formation.

LL_{DI}, LL_B, and LL_K of xanthan gum–treated montmorillonite–sand soils

For montmorillonite–sand soils, LL_{DI} decreases gradually with xanthan gum content (Fig. 4*a*). Montmorillonite shows high hydrophilicity owing to its high SSA and CEC, where xanthan gum hydrogel seems to have less effect on the variation in pore-fluid viscosity, while xanthan gum–induced montmorillonite aggregation seems to be the main factor decreasing LL_{DI}. The edge sites of montmorillonite are regarded as negligible owing to the low thickness-to-length ratio (<0.01) (Santamarina et al. 2001; Secor and Radke 1985), where xanthan gum can mainly interact within the interlayer spaces of montmorillonite (Deng et al. 2006; Laird 1997; Theng 2012) or form hydrogen bonds with water molecules in the Gouy diffuse layer (Ng and Plank 2012), resulting in the reduction of the double-layer thickness and accompanying LL_{DI}

Fig. 4. Liquid limit of xanthan gum–treated montmorillonite–sand soils with variation in m_b/m_s: (a) deionized water pore fluid; (b) 2 mol/L NaCl brine pore fluid; (c) kerosene pore fluid.

Fig. 5. Liquid limit increment by xanthan gum content in brine condition.

clayey soils from LL_{DI} to LL_B (Figs. 3 and 4), while silt shows no effect ($LL_{DI} \approx LL_B$; Fig. 2). Figure 5 expresses the increment in LL_B of soils ($LL_{B,X\%} - LL_{B,0\%}$) according to xanthan gum treatment, where $LL_{B,X\%}$ denotes the LL_B at $X\%$ xanthan gum treatment and $LL_{B,0\%}$ denotes the LL_B of untreated soils. A similar increase in LL_B with xanthan gum treatment, regardless of the soil type, implies that xanthan gum mainly forms hydrogels that can be attributed to the increase in viscosity of pore fluids (Nugent et al. 2009) or interacting with concentrated Na+ ions in the reduced double-layer under brine pore-fluid conditions (Theng 2012).

The insignificant variation in LL_K with xanthan gum treatment, shown in Figs. 2c, 3c, and 4c, implies the importance of water for the hydrogel formation of xanthan gum and the accompanying interactions with soil particles and pore fluids. Thus, it can be concluded that hydrogel formation is an important prerequisite for xanthan gum in soil treatment and ground improvement practices.

Xanthan gum biopolymer – pore-fluid effect on classification of soils

Fine-grained soils (L10, L5S5, K10, K5S5, M10, and M5S5) used in this study were plotted on the LL–PI plane (Fig. 6a). Xanthan gum treatment in clayey silt tends to increase both LL and PI, which alters the Unified Soil Classification System (USCS; ASTM 2017b) classification from ML to CL. Both the LL and PI of kaolinite-based soils instantly increase at low xanthan gum contents ($m_b/m_s = 0.5\%$ for K10; $m_b/m_s = 0.25\%$ for K5S5) and decrease at higher xanthan gum contents. Most kaolinite-based soils are classified as clay (CH for K10; CL for K5S5), while some are classified as silt (e.g., MH for K10 with $m_b/m_s = 1\%$; ML for K5S5 with $m_b/m_s = 1\%$). Montmorillonite-based soils are classified as clay with high plasticity (CH), regardless of the content of xanthan gum, while both LL and PI tends to decrease with xanthan gum treatment.

Meanwhile, as xanthan gum treatment seems to alter the USCS classification of fine soils, the pore-fluid effect (e.g., pH, electrical conductivity, and permittivity) has been considered based on the electrical sensitivity (S_E) and LL_B values according to Jang and Santamarina (2016).

Figure 6b displays all soils used in this study plotted on the S_E–LL_B chart with similar references (silica flour, kaolinite-based soils, montmorillonite-based soils) from previous studies (Jang and Santamarina 2016; Park and Santamarina 2017). LL_B distinguishes the plasticity of soils from none to high plasticity, while S_E is classified into low, intermediate, and high S_E conditions (Fig. 6b). Both the plasticity and S_E increase with higher clay contents and soil type variations in the following order: clayey silt → kaolinite → montmorillonite. Xanthan gum treatment induces an increase in soil plasticity owing to the formation of viscous hy-

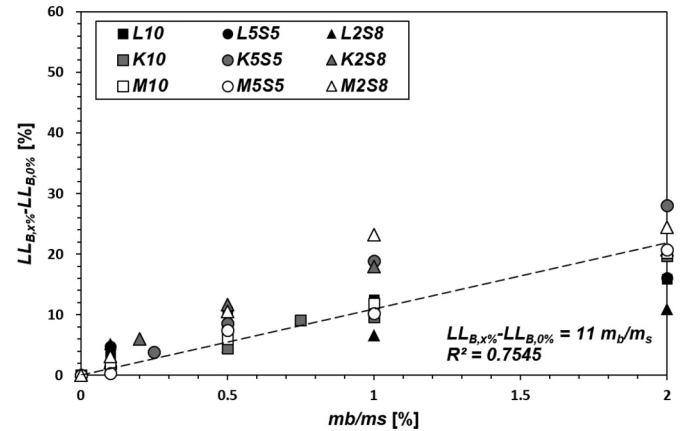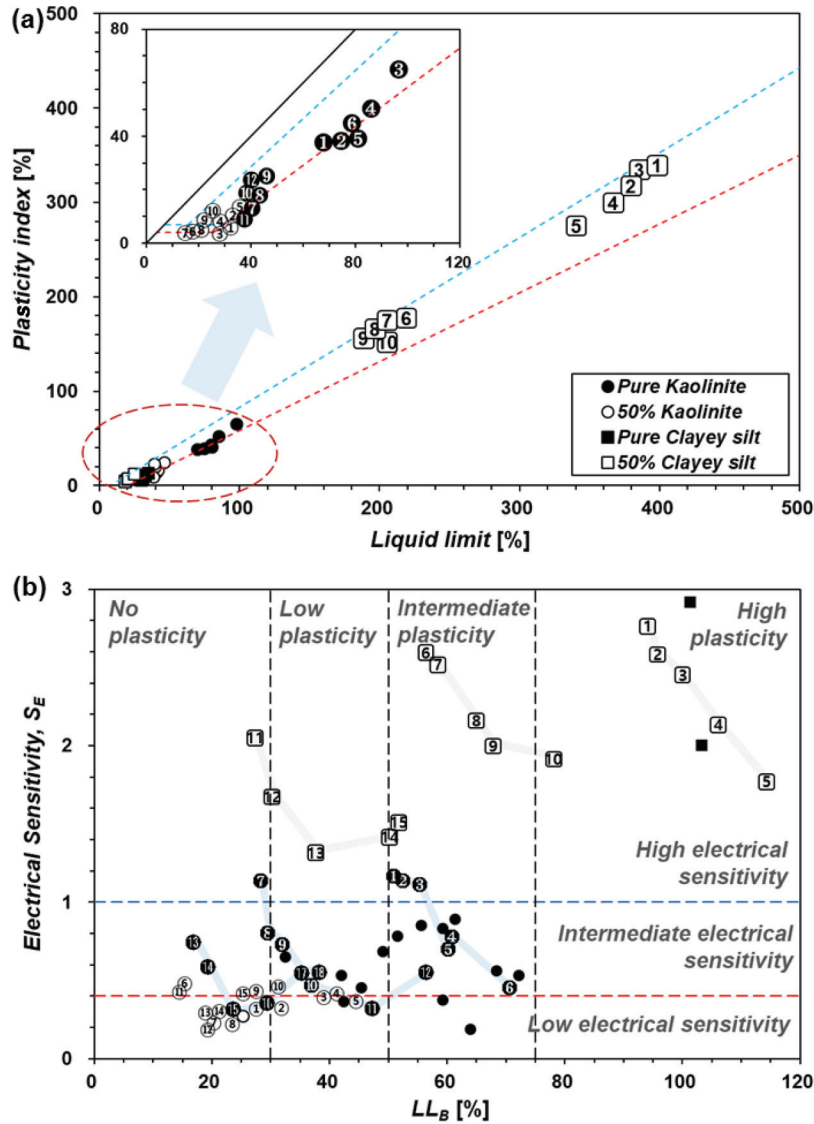decrement with xanthan gum content (Fig. 4a) (Hayes and Swift 1978; Rao et al. 1993).

Meanwhile, LL_B (Fig. 4b) follows similar behaviors under relevant pore-fluid conditions of clayey silt–sand and kaolinite-sand soils. Xanthan gum does not seem to have any effect on LL_K (Fig. 4c), similar to other types of soils.

Discussion

LL behavior of xanthan gum–treated fine soils with pore-fluid variation

The effect of xanthan gum on LL_{DI} varies with different soil types, as shown in Figs. 3–5. Brine pore fluid reduces the LL of

Fig. 6. Chart for classification of soils used in this study (*a*) based on USCS and (*b*) based on electrical sensitivity and liquid limits in brine. Numbered points, xanthan gum-treated soils; empty circles, silica flour (Jang and Santamarina 2016); filled circles: kaolinite-based soils (Park and Santamarina 2017); squares, montmorillonite-based soils (Park and Santamarina 2017). [Color online.]

	0	0.1	0.2	0.25	0.5	0.75	1	2
Pure Clayey silt (L10)	①	②			③		④	⑤
50% Clayey silt (L5S5)	⑥	⑦			⑧		⑨	⑩
20% Clayey silt (L2S8)	⑪	⑫			⑬		⑭	⑮
Pure Kaolinite (K10)	❶	❷			❸	❹	❺	❻
50% Kaolinite (K5S5)	❼	❽		❾	❿		⓫	⓬
20% Kaolinite (K2S8)	⓭	⓮	⓯		⓰		⓱	⓲
Pure Montmorillonite (M10)	1	2			3		4	5
50% Montmorillonite (M5S5)	6	7			8		9	10
20% Montmorillonite (M2S8)	11	12			13		14	15

drogel when using brine pore fluid, while S_E initially decreases and then increases with xanthan gum contents.

The values of S_E of clayey silt–sand soils are mainly low, while in some cases, these values are found near the boundary between intermediate and low S_E. For kaolinite–sand soils, the minimum S_E is observed at a m_b/m_s of 0.2%, 1%, and 2% for K2S8, K5S5, and K10 soils, respectively. With respect to xanthan gum–to-clay mass content (m_b/m_c), the lowest S_E points are observed at m_b/m_c values of 1%, 2%, and 2% for K2S8, K5S5, and K10 soils, respectively. For montmorillonite–sand soils, S_E decreases up to $m_b/m_c = 4\%$ (2%

xanthan gum content in M5S5). The overall S_E reduction of clays (K10, K5S5, M10, M5S5) with xanthan gum treatment seems to be related to xanthan gum–induced clay particle aggregation, where an advanced technique (e.g., liquid-cell microscopy on aqueous phase xanthan gum – clay – pore fluids) can be used for further investigation.

Conclusion

Pore-fluid chemistry and clay-mineral type are salient factors in xanthan gum biopolymer treatment in fine soils. However, xan-

than gum behavior variations according to the pore-fluid chemistry and clay mineral have not been analyzed in previous studies. Therefore, this study addresses this gap in the research.

Liquid limits of xanthan gum–treated soils were measured using chemically distinctive pore fluids. Under deionized-water conditions, xanthan gum behavior was affected by the clay type. With the clayey silt, xanthan gum formed viscous hydrogel in the pore space among clay particles, and LL_{DI} was increased as xanthan gum–clay content increased. With kaolinite, LL_{DI} peaked at a xanthan gum–clay content of 0.5%, and decreased until a content of 1.0% was reached, which implies the simultaneous hydrogel formation in pores and particle aggregation induced by xanthan gum. With montmorillonite, LL_{DI} decreased gradually with an increase in xanthan gum–clay content, which implies xanthan gum mainly aggregates montmorillonite particles rather than affecting the viscosity of the pore fluid. The overall electrical sensitivity reduction with xanthan gum treatment implies that interparticle aggregation is the main phenomenon of clays at low xanthan gum–clay contents. In contrast, xanthan gum behavior was governed by pore-fluid chemistry in brine and kerosene conditions, regardless of clay type. With brine, counter-ions decreased LL_B of clays significantly, while LL_B tended to increase with higher xanthan gum–clay content. For kerosene, LL_K showed no remarkable changes with xanthan gum treatment.

Acknowledgement

References

ASTM. 2007. Standard test methods for laboratory determination of water (moisture) content of soil and rock by mass. ASTM standard D2216-05. ASTM International, West Conshohocken, Pa. pp. 210–216. doi:10.1520/D2216-05.

ASTM. 2017a. Standard test methods for liquid limit, plastic limit, and plasticity index of soils. ASTM standard D4318-17. In ASTM Volume 04.08 Soil and Rock (I): D421–D5876. ASTM International, West Conshohocken, Pa. pp. 542–557. doi:10.1520/D4318-17.

ASTM. 2017b. Standard practice for classification of soils for engineering purposes (Unified Soil Classification System). ASTM standard D2487. ASTM International, West Conshohocken, Pa. doi:10.1520/D2487-17.

Awad, Y.M., Blagodatskaya, E., Ok, Y.S., and Kuzyakov, Y. 2012. Effects of polyacrylamide, biopolymer, and biochar on decomposition of soil organic matter and plant residues as determined by 14C and enzyme activities. European Journal of Soil Biology, 48: 1–10. doi:10.1016/j.ejsobi.2011.09.005.

Brady, P.V., Cygan, R.T., and Nagy, K.L. 1996. Molecular controls on kaolinite surface charge. Journal of Colloid and Interface Science, 183(2): 356–364. doi:10.1006/jcis.1996.0557. PMID:8954678.

British Standards Institution. 2017. BS EN ISO 17892: Geotechnical investigation and testing - Laboratory testing of soil. Part 6: Fall cone test. British Standards Institution. doi:10.3403/30304213U.

Cabalar, A.F., Wiszniewski, M., and Skutnik, Z. 2017. Effects of xanthan gum biopolymer on the permeability, odometer, unconfined compressive and triaxial shear behavior of a sand. Soil Mechanics and Foundation Engineering, 54(5): 356–361. doi:10.1007/s11204-017-9481-1.

Chang, I., and Cho, G.-C. 2010. A new alternative for estimation of geotechnical engineering parameters in reclaimed clays by using shear wave velocity. Geotechnical Testing Journal, 33(3): 171–182. doi:10.1520/GTJ102360.

Chang, I., and Cho, G.-C. 2012. Strengthening of Korean residual soil with β-1,3/1,6-glucan biopolymer. Construction and Building Materials, 30(0): 30–35. doi:10.1016/j.conbuildmat.2011.11.030.

Chang, I., and Cho, G.-C. 2014. Geotechnical behavior of a beta-1,3/1,6-glucan biopolymer-treated residual soil. Geomechanics and Engineering, 7(6): 633–647. doi:10.12989/gae.2014.7.6.633.

Chang, I., and Cho, G.-C. 2019. Shear strength behavior and parameters of microbial gellan gum-treated soils: from sand to clay, Acta Geotechnica, 14(2): 361–375. doi:10.1007/s11440-018-0641-x.

Chang, I., Im, J., Prasidhi, A.K., and Cho, G.-C. 2015a. Effects of Xanthan gum

biopolymer on soil strengthening. Construction and Building Materials, 74(0): 65–72. doi:10.1016/j.conbuildmat.2014.10.026.

Chang, I., Jeon, M., and Cho, G.-C. 2015b. Application of microbial biopolymers as an alternative construction binder for earth buildings in underdeveloped countries. International Journal of Polymer Science, 2015: 9. doi:10.1155/2015/326745.

Chang, I., Prasidhi, A.K., Im, J., and Cho, G.-C. 2015c. Soil strengthening using thermo-gelation biopolymers. Construction and Building Materials, 77: 430–438. doi:10.1016/j.conbuildmat.2014.12.116.

Chang, I., Prasidhi, A.K., Im, J., Shin, H.-D., and Cho, G.-C. 2015d. Soil treatment using microbial biopolymers for anti-desertification purposes. Geoderma, 253–254: 39–47. doi:10.1016/j.geoderma.2015.04.006.

Chang, I., Im, J., and Cho, G.-C. 2016a. Geotechnical engineering behaviors of gellan gum biopolymer treated sand. Canadian Geotechnical Journal, 53(10): 1658–1670. doi:10.1139/cgj-2015-0475.

Chang, I., Im, J., and Cho, G.C. 2016b. Introduction of microbial biopolymers in soil treatment for future environmentally-friendly and sustainable geotechnical engineering. Sustainability, 8(3): 251. doi:10.3390/su8030251.

Chang, I., Im, J., Lee, S.-W., and Cho, G.-C. 2017. Strength durability of gellan gum biopolymer-treated Korean sand with cyclic wetting and drying. Construction and Building Materials, 143: 210–221. doi:10.1016/j.conbuildmat.2017.02.061.

Chang, I., Im, J., Chung, M.-K., and Cho, G.-C. 2018. Bovine casein as a new soil strengthening binder from diary wastes. Construction and Building Materials, 160: 1–9. doi:10.1016/j.conbuildmat.2017.11.009.

Chen, R., Lee, I., and Zhang, L. 2015. Biopolymer stabilization of mine tailings for dust control. Journal of Geotechnical and Geoenvironmental Engineering, 141(2): 04014100. doi:10.1061/(ASCE)GT.1943-5606.0001240.

Das, B.M. 2013. Advanced soil mechanics. CRC Press.

Deng, Y., Dixon, J.B., and White, G.N. 2006. Adsorption of polyacrylamide on smectite, illite, and kaolinite. Soil Science Society of America Journal, 70(1): 297–304. doi:10.2136/sssaj2005.0200.

Dove, C.A., Bradley, F.F., and Patwardhan, S.V. 2016. Seaweed biopolymers as additives for unfired clay bricks. Materials and Structures, 49(11): 4463–4482. doi:10.1617/s11527-016-0801-0.

Ferruzzi, G.G., Pan, N., and Casey, W.H. 2000. Mechanical properties of gellan and polyacrylamide gels with implications for soil stabilization. Soil Science, 165(10): 778–792. doi:10.1097/00010694-200010000-00003.

García-Ochoa, F., Santos, V.E., Casas, J.A., and Gómez, E. 2000. Xanthan gum: production, recovery, and properties. Biotechnology Advances, 18(7): 549–579. doi:10.1016/S0734-9750(00)00050-1. PMID:14538095.

Ham, S., Kwon, T., Chang, I., and Chung, M. 2016. Ultrasonic P-wave reflection monitoring of soil erosion for erosion function apparatus. Geotechnical Testing Journal, 39(2): 301–314. doi:10.1520/GTJ20150040.

Ham, S.-M., Chang, I., Noh, D.-H., Kwon, T.-H., and Muhunthan, B. 2018. Improvement of surface erosion resistance of sand by microbial biopolymer formation. Journal of Geotechnical and Geoenvironmental Engineering, 144(7): 06018004. doi:10.1061/(ASCE)GT.1943-5606.0001900.

Hansbo, S. 1957. A new approach to the determination of the shear strength of clay by the fall-cone test. Royal Swedish Geotechnical Institute.

Hayes, M.H.B., and Swift, R.S. 1978. The chemistry of soil organic colloids. In The chemistry of soil constituents. Edited by D.J. Greenland and M.H.B. Hayes. Wiley, New York. pp. 179–320.

Hensen, E.J.M., and Smit, B. 2002. Why Clays Swell. The Journal of Physical Chemistry B, 106(49): 12664–12667. doi:10.1021/jp0264883.

Im, J., Tran, A.T.P., Chang, I., and Cho, G.-C. 2017. Dynamic properties of gel-type biopolymer-treated sands evaluated by Resonant Column (RC) tests. Geomechanics and Engineering, 12(5): 815–830. doi:10.12989/gae.2017.12.5.815.

Inglethorpe, S.D.J., Morgan, D.J., Highley, D.E., and Bloodworth, A.J. 1993. Industrial minerals laboratory manual: bentonite. British Geological Survey.

Jang, J., and Santamarina, J.C. 2016. Fines classification based on sensitivity to pore-fluid chemistry. Journal of Geotechnical and Geoenvironmental Engineering, 142(4). doi:10.1061/(ASCE)GT.1943-5606.0001420.

Kim, K.Y., Yun, T.S., and Park, K.P. 2013. Evaluation of pore structures and cracking in cement paste exposed to elevated temperatures by X-ray computed tomography. Cement and Concrete Research, 50: 34–40. doi:10.1016/j.cemconres.2013.03.020.

Koumoto, T., and Houlsby, G.T. 2001. Theory and practice of the fall cone test. Géotechnique, 51(8): 701–712. doi:10.1680/geot.2001.51.8.701.

Kwon, T.-H., and Ajo-Franklin, J.B. 2013. High-frequency seismic response during permeability reduction due to biopolymer clogging in unconsolidated porous media. Geophysics, 78(6): EN117–EN127. doi:10.1190/geo2012-0392.1.

Laird, D.A. 1997. Bonding between polyacrylamide and clay mineral surfaces. Soil Science, 162(11): 826–832. doi:10.1097/00010694-199711000-00006.

Latifi, N., Horpibulsuk, S., Meehan, C.L., Majid, M.Z.A., Tahir, M.M., and Mohamad, E.T. 2017. Improvement of problematic soils with biopolymer - An environmentally friendly soil stabilizer. Journal of Materials in Civil Engineering, 29(2). doi:10.1061/(ASCE)MT.1943-5533.0001706.

Lee, S., Chang, I., Chung, M.-K., Kim, Y., and Kee, J. 2017. Geotechnical shear behavior of xanthan gum biopolymer treated sand from direct shear testing. Geomechanics and Engineering, 12(5): 831–847. doi:10.12989/gae.2017.12.5.831.

Martin, G., Yen, T., and Karimi, S. 1996. Application of biopolymer technology in silty soil matrices to form impervious barriers. *In* 7th Australia New Zealand Conference on Geomechanics: Geomechanics in a Changing World: Conference Proceedings, Institution of Engineers, Australia, p. 814.

Mitchell, J.K., and Soga, K. 2005. Fundamentals of soil behavior. 3rd ed. John Wiley & Sons, Hoboken, N.J.

Ng, S., and Plank, J. 2012. Interaction mechanisms between Na montmorillonite clay and MPEG-based polycarboxylate superplasticizers. Cement and Concrete Research, **42**(6): 847–854. doi:10.1016/j.cemconres.2012.03.005.

Nugent, R.A., Zhang, G., and Gambrell, R.P. 2009. Effect of exopolymers on the liquid limit of clays and its engineering implications. Transportation Research Record: Journal of the Transportation Research Record, **2101**: 34–43. doi:10.3141/2101-05.

Orts, W.J., Sojka, R.E., and Glenn, G.M. 2000. Biopolymer additives to reduce erosion-induced soil losses during irrigation. Industrial Crops and Products, **11**(1): 19–29. doi:10.1016/S0926-6690(99)00030-8.

Orts, W., Roa-Espinosa, A., Sojka, R., Glenn, G., Imam, S., Erlacher, K., and Pedersen, J. 2007. Use of synthetic polymers and biopolymers for soil stabilization in agricultural, construction, and military applications. Journal of Materials in Civil Engineering, **19**(1): 58–66. doi:10.1061/(ASCE)0899-1561(2007)19:1(58).

Park, J., and Santamarina, J.C. 2017. Revised soil classification system RSCS. *In* Proceedings of the 19th International Conference on Soil Mechanics and Geotechnical Engineering, Seoul, pp. 1081–1084.

Plaschke, M., Schäfer, T., Bundschuh, T., Ngo Manh, T., Knopp, R., Geckeis, H., and Kim, J. 2001. Size characterization of bentonite colloids by different methods. Analytical Chemistry, **73**(17): 4338–4347.

Qureshi, M.U., Chang, I., and Al-Sadarani, K. 2017. Strength and durability characteristics of biopolymer-treated desert sand. Geomechanics and Engineering, **12**(5): 785–801. doi:10.12989/gae.2017.12.5.785.

Rao, S.M., Sridharan, A., and Shenoy, M.R. 1993. Influence of starch polysaccharide on the remoulded properties of two Indian clay samples. Canadian Geotechnical Journal, **30**(3): 550–553. doi:10.1139/t93-047.

Santamarina, J.C., Klein, K.A., and Fam, M.A. 2001. Soils and waves. J. Wiley & Sons, Chichester, New York.

Sastry, N.V., Séquaris, J.M., and Schwuger, M.J. 1995. Adsorption of polyacrylic acid and sodium dodecylbenzenesulfonate on kaolinite. Journal of Colloid and Interface Science, **171**(1): 224–233. doi:10.1006/jcis.1995.1171.

Secor, R.B., and Radke, C.J. 1985. Spillover of the diffuse double layer on montmorillonite particles. Journal of Colloid and Interface Science, **103**(1): 237–244. doi:10.1016/0021-9797(85)90096-7.

Sondi, I., Bišćan, J., and Pravdić, V. 1996. Electrokinetics of pure clay minerals revisited. Journal of Colloid and Interface Science, **178**(2): 514–522. doi:10.1006/jcis.1996.0146.

Sridharan, A., and Prakash, K. 1999. Mechanisms controlling the undrained shear strength behaviour of clays. Canadian Geotechnical Journal, **36**(6): 1030–1038. doi:10.1139/t99-071.

Sridharan, A., Rao, S., and Murthy, N. 1986. Liquid limit of montmorillonite soils. Geotechnical Testing Journal, **9**(3): 156–159. doi:10.1520/GTJ10623J.

Sridharan, A., Rao, S.M., and Murthy, N.S. 1988. Liquid limit of kaolinitic soils. Géotechnique, **38**(2): 191–198. doi:10.1680/geot.1988.38.2.191.

Taylor, R.K. 1985. Cation exchange in clays and mudrocks by methylene blue. Journal of Chemical Technology and Biotechnology, **35**(4): 195–207. doi:10.1002/jctb.5040350407.

Theng, B.K.G. 2012. Formation and properties of clay–polymer complexes. Elsevier.

Tombácz, E., and Szekeres, M. 2006. Surface charge heterogeneity of kaolinite in aqueous suspension in comparison with montmorillonite. Applied Clay Science, **34**(1–4): 105–124. doi:10.1016/j.clay.2006.05.009.

White, W.A. 1949. Atterberg plastic limits of clay minerals. American Mineralogist, **34**(7–8): 508–512.

List of symbols

CEC	cation-exchange capacity
D_{50}	mean grain size
LL	liquid limit of soils
LL_B	liquid limit of soils with 2 mol/L NaCl brine pore fluid obtained by laboratory fall cone test
LL_{DI}	liquid limit of soils with deionized water pore fluid obtained by laboratory fall cone test
LL_K	liquid limit of soils with kerosene pore fluid obtained by laboratory fall cone test
m_b	mass of biopolymer (xanthan gum, in this study)
m_b/m_c	xanthan gum–to-clay ratio in mass
m_b/m_s	xanthan gum–to-soil ratio in mass
m_c	mass of clay
m_s	mass of soil
PL	plastic limit of soils
PI	plasticity index (LL – PL) of soils
S_E	electrical sensitivity
SSA	specific surface area of soil particles (m²/g)
κ'	relative permittivity
σ_{el}	electric conductivity